Heliyon 10 (2024) e28027

Contents lists available at ScienceDirect

Heliyon

journal homepage: www.cell.com/heliyon

Research article

Therapeutic potential of Thai herbal formula for cognitive impairment: A metabolomics approach for Comprehensive Insights

Pravit Akarasereenont [a,c,e,*], Saracha Pattanapholkornsakul [a], Suveerawan Limsuvan [a], Dollaporn Mamaethong [a], Suksalin Booranasubkajorn [a], Narawut Pakaprot [b], Pinpat Tripatara [c], Kajee Pilakasiri [d]

[a] Center of Applied Thai Traditional Medicine, Faculty of Medicine Siriraj Hospital, Mahidol University, 10700, Bangkok, Thailand
[b] Department of Physiology, Faculty of Medicine Siriraj Hospital, Mahidol University, 10700, Bangkok, Thailand
[c] Department of Pharmacology, Faculty of Medicine Siriraj Hospital, Mahidol University, 10700, Bangkok, Thailand
[d] Department of Anatomy, Faculty of Medicine Siriraj Hospital, Mahidol University, 10700, Bangkok, Thailand
[e] Siriraj Metabolomics and Phenomics Center, Faculty of Medicine Siriraj Hospital, Mahidol University, 10700, Bangkok, Thailand

ARTICLE INFO

Keywords:
YAHOM20
YHF20
Cerebral ischemia
Metabolomics
Cognitive impairment
Thai herbal formula

ABSTRACT

Chronic cerebral ischemia hypoperfusion plays a role in the initiation and progression of vascular dementia, which causes changes in metabolites. Currently, there is no standard treatment to treat, prevent and reduce the severity of this condition. Thai herbal Yahom no.20 (YHF20) is indicated for fatigue and dizziness. The components of YHF20 have been found to have pharmacological effects related to the pathology of chronic cerebral ischemia hypoperfusion. This study aimed to investigate metabolomic changes after YHF20 administration in a rat model of permanent bilateral common carotid artery occlusion (2-VO) induced chronic cerebral ischemia hypoperfusion, and to explore its impact on spatial learning and memory. Albino Wistar rats were randomly allocated to 5 groups; sham, 2-VO, 2-VO+ 100 mg/kg YHF20, 2-VO+300 mg/kg YHF20, and 2-VO+1000 mg/kg YHF20. The rats were administered YHF20 daily by oral gavage for 56 days after 2-VO induction. Plasma was collected weekly for metabolome change analysis using LC-MS/QTof and toxicity study. The rats were evaluated for spatial learning and memory using the Morris water maze. The results showed that 78 known metabolites and 10 tentative pathways altered after chronic cerebral hypoperfusion, although it was not able to determine the effect on memory and learning behaviors of rats. Glutathione and glutathione metabolism might be metabolite-pathway that were the affect after YHF20 administration in cerebral ischemic condition. The 4 known metabolites may be the metabolites from the constituents of YHF20 could be considered and confirmed for quality control purpose. In conclusion, YHF20 administration might contribute to metabolic changes related to cerebral ischemia condition without the effect on spatial learning and memory, including hepatotoxicity and nephrotoxicity after 56 days of

* Corresponding author. Center of Applied Thai Traditional Medicine, Faculty of Medicine Siriraj Hospital, Mahidol University, 10700, Bangkok, Thailand.

E-mail addresses: pravit.auk@mahidol.ac.th (P. Akarasereenont), saracha.pat@mahidol.edu (S. Pattanapholkornsakul), suveerawan.lim@mahidol.edu (S. Limsuvan), dollaporn.mam@mahidol.edu (D. Mamaethong), suksakin.boo@mahidol.edu (S. Booranasubkajorn), narawut.pak@mahidol.ac.th (N. Pakaprot), pinpat.tri@mahidol.edu (P. Tripatara), kpilakasiri5@yahoo.com (K. Pilakasiri).

https://doi.org/10.1016/j.heliyon.2024.e28027
Received 29 November 2023; Received in revised form 9 March 2024; Accepted 11 March 2024
Available online 16 March 2024

treatment. Alterations in the potential metabolites may provide data support for elucidating dementia pathogenesis and selecting pathways for intervention.

1. Introduction

Dementia is characterized by multiple cognitive deficits, including memory loss, decline in thinking skills, and emotional and language problems. The most common types of dementia are Alzheimer's disease (AD) and vascular dementia (VaD), respectively. VaD is a pathophysiological condition resulting in a sudden and progressive decline in cognitive and memory function caused by inadequate blood flow to the brain [1]. Etiology of VaD is unclear. Previous studies showed the chronic reduction of cerebral blood flow, which is found in aging and neurodegenerative disorders, was associated with cognitive deficit [2,3]. athologies such as neuronal death (mostly apoptosis), inflammation, and oxidative stress occur when there is the chronic reduction of cerebral blood flow [4]. The evidence suggests that chronic cerebral hypoperfusion is essential in the initiation and progression of VaD. Many animal models have been created to simulate cerebral blood flow impairment conditions, which are manipulated in acute or slow, complete or incomplete, focal or global, and permanent or transient reductions. The experimental ischemic models comprise focal ischemic, global ischemic [5,6], and hypoperfusion models [5]. This study will focus on learning and memory impairment caused by chronic cerebral hypoperfusion. Memory loss in dementia was associated with explicit memory. The encoding and storages of explicit information are due to the activity of the prefrontal cortex and hippocampus. The prefrontal cortex is associated with working memory that could change to short-term memory. When we need to recall the information, we could change short-term memory to long-term memory. The transformation mechanism was called the consolidation process in which the hippocampus is an important region that plays a critical role in this process. Hippocampal-dependent learning and memory assessment has many tests such as radial arm maze, Barnes maze, Morris water maze, contextual fear conditioning test, object location memory test, etc [7]. The Morris water maze is widely used for evaluating behavioral and cognitive abilities in rodents because it is a well-validated test that assesses spatial learning and memory.

YHF20 is a herbal formulation that contains 25 components (Table S1) as follows *Amomum testaceum* Rid., *Aquilaria malaccensis* Lam., *Euphorbia antiquorum* L., *Syzygium aromaticum* (L.) Merr. & L.M. Perry, *Artemisia pallens* Wall. Ex DC., *Angelica sinensis* (Oliv.) Diels., *Terminalia chebula* Retz. Var. chebula, *Ligusticum sinense* Oliv. Cv. Chuanxiong, *Mimusops elengi* L., *Dracaena Loureirin* Gagnep., *Myristica fragrans* Houtt., *Alyxia reinwardtii* Blume, *Glycyrrhiza glabra* L., *Nelumbo nucifera* Gaertn., *Mesua ferrea* L., *Vetiveria zizanioides* (L.) Nash ex Small, *Urceola rosea* (Hook. & Arn.) D.J.Middleton, *Cinnamomum bejolghota* (Buch.-Ham.) Sweet, *Mammea siamensis* Kosterm., *Cinnamomum verum* J.S. Presl., *Cinnamomum loureirii* Nees., Sodium borate and Borneo Camphor; their pictures are shown in Supplementary Material, Fig S1. The proportions of components are equal. YHF20 is often used for the relief of symptoms like nausea, vomiting, dizziness, fatigue, and insufficient sleep. Many components of YHF20 have been reported for pharmacological activities related to the hemodynamic system [8–14], vasodilatation [13,15], antioxidation [16–23], and anti-inflammation [24–31] (Table S1). Thus, the present study was designed to investigate metabolomics changes after YHF20 administration in ischemic rats and to explore its impact on spatial learning and memory.

2. Materials and methods

2.1. Materials and reagents

YHF20 powder was obtained from Herbal Medicines and Products Manufacturing Unit, manufactured under Good Manufacturing Practice (GMP) PIC/s by Ayurved Siriraj, Center of Applied Thai Traditional Medicine, Faculty of Medicine Siriraj Hospital, Mahidol University, Thailand. YHF20 was verified for quality control using LC-MS by comparing the chromatogram fingerprint of each production batch from manufacturing unit. The chromatogram of YHF20 is shown in Supplementary Material, Fig S2. Alanine aminotransferase (ALT), aspartate aminotransferase (AST), urea/BUN-UV, and creatinine were purchased from Biosystems (Spain). All chemicals used were optima® LC-MS grade in metabolic profile analysis. For the animal study, YHF20 was suspended in sterile water.

2.2. Experimental animals

Seventy-eight adult (7 weeks) male Wistar rats (weight between 200 and 250 g) were used in all experiments. All animals were obtained from Nomura Siam International Co, Ltd., Pathumwan, Bangkok, Thailand. They were maintained in the 12-h light/dark cycle and were housed in individual ventilated cage with Ad libitum standard diet and sterile distilled water at Siriraj Laboratory Animal Research and Care Center. They were acclimatized for 2 weeks before the experiments.

2.3. Establishment of permanent bilateral common carotid occlusion (pBCCAO)

The rats were anesthetized by intramuscular injection of ketamine (60 mg/kg) and xylazine (6.0 mg/kg). The unconscious rats were placed onto a controlled heating pad and then body temperature was monitored. The rats were incised at the midline of the neck region. Both common carotid arteries were dissected and carefully separated from the vagus nerve. Both common carotid arteries were ligated with silk suture before suturing the incision. The suture area was applied with antibiotic ointment and xylocaine 2% gel, respectively. The rats were subcutaneously injected with carprofen 5 mg/kg 2 times to relief pain. Post-surgery, rats were kept under

observation and a heating lamp until recovery from anesthesia. The rats were returned to the cage when they fully regained consciousness.

2.4. Animal grouping and drug administration

The rats were randomly allocated into 5 different groups which were the sham-operated group (sham), the vehicle-treated bilateral common carotid artery-occluded group (2-VO + vehicle), the 100 mg/kg of YHF20 vehicle-treated bilateral common carotid artery-occluded group (2-VO+100 mg/kg YHF20), the 300 mg/kg of YHF20 vehicle-treated bilateral common carotid artery-occluded group (2-VO+300 mg/kg YHF20), and the 1000 mg/kg of YHF20 vehicle-treated bilateral common carotid artery-occluded group (2-VO+1000 mg/kg YHF20). The YHF20 doses were converted from clinical doses by the equivalent dose ratio between body surface areas of human and animals. Each group daily received sterile water or YHF20 by oral gavage for 8 weeks (Fig. 1). Then, the first day of administration started within 24 h after pBCCAO.

2.5. Blood collection and preparation

The rats blood were collected in heparin tubes from the lateral tail vein using a butterfly needle (23G) at day 1, 9, 16, 23, 30, 37, 44, 51, and 58. Blood samples were centrifuged (8000 g for 10 min at 4 °C) to separate plasma. All plasma samples were stored at −80 °C within 4 h and were used for metabolic profiles analysis and biochemical analysis (Fig. 1).

2.6. Sample preparation for metabolic profiles analysis

Plasma was thawed at room temperature until completely melt. It was centrifuged at 4000 g 10 min 4 °C. Supernatant was divided as sample, pooled qc, and pooled group. Then, MeOH (700 μL) and internal standard (25 μL) were pipetted into plasma, mixed using vortex for 10 s, and continued mixed using a shaker at 2000 rpm for 15 min. After that, samples were stored at −80 °C for 60 min. Then, samples were centrifuged at 18,000 g for 10 min at 4 °C. The supernatant was pipetted as samples (300 μL) and technical QC (TQC). The supernatant was concentrated by SpeedVac concentrator until samples were completely dry and were stored at −80 °C until

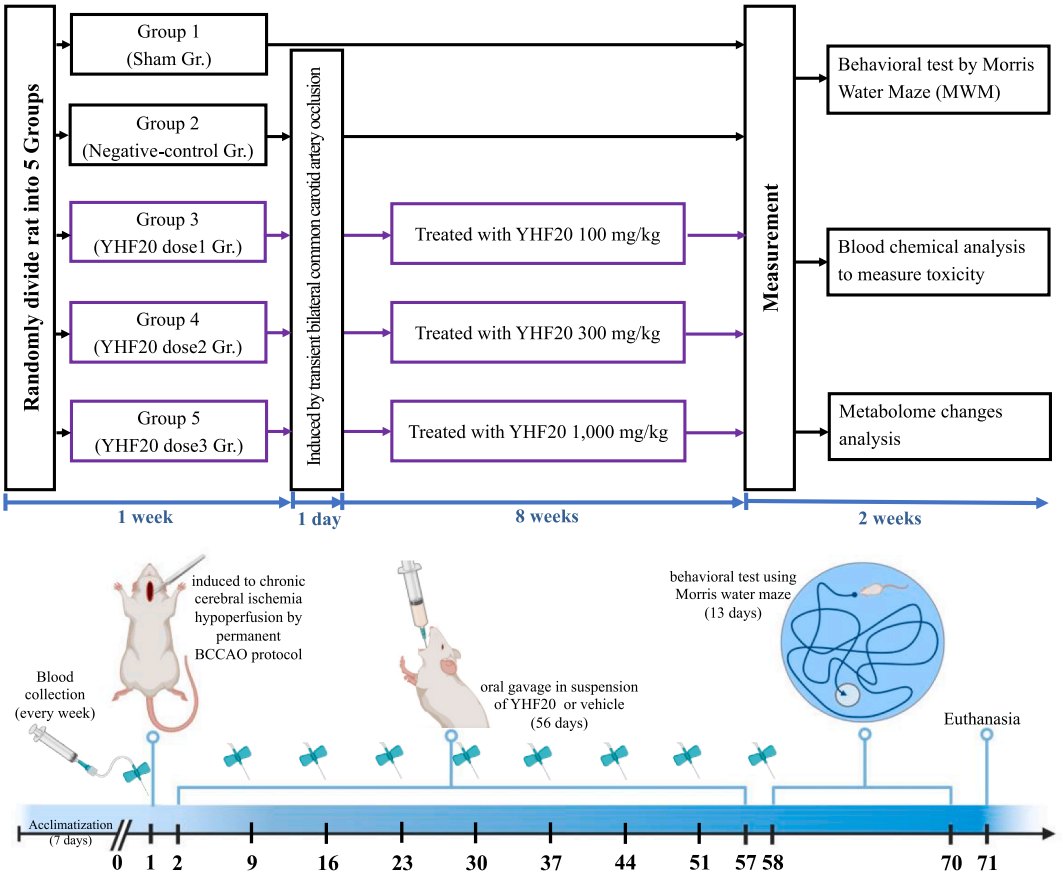

Fig. 1. Experimental protocol.

analysis. Samples were reconstituted with Milli-Q water (100 mL) and were centrifuged 15,800 g at 4 °C for 15 times. In all steps, samples were placed on the cold rack (~4 °C) except SpeedVac concentrating. The supernatant was used to determine the metabolic profiles using LC-MS-QtoF.

2.7. Metabolic profile analysis

The chromatographic separation was performed with AQUITY UPLC HSS T3 (1.8 μm, 2.1 × 100 mm) column with guard column coupling binary solvent system and auto-sampler. The column temperature was maintained at 40 °C. The sample temperature was 4 °C. The injection volume was 5 μL. The mobile phase was consisted of 0.1% Formic acid in Milli-Q water (A) and 0.1% Formic acid in MeOH (B) at a flow rate of 0.4 mL/min. The condition was linear-gradient (curve 6) elution as follows: kept 100%A 0%B at 0–1 min for equilibration (1 min), in next changed to 0%A 100%B at 1–16 min (15 min) for analysis and maintained to washing column at 16–20 min (4 min), recondition to 100%A 0%B at 20–22 min (2 min), and maintained at 22–24 min (2 min). The total run time was 24 min per analysis. Mass spectrometry detection was performed on SYNAPT G2-Si HDMS QTOF (Waters Corp., MA, USA) equipped with electrospray ionization (ESI) interference. The analysis was in positive mode and negative mode using Mse analysis mode. Acquisition time was 24 min in the resolution analyzer mode. The mass range was 100–1200 Da with continuum scanning (0.5 s). Low collision energy for precursor analysis was set at 4 V but high collision energy was performed at 20–40 V for fragment ions. The parameters were capillary voltage of 3 kV, sampling cone voltage of 40 V, source offset of 80 V, source temperature of 150 °C, and desolvation temperature of 500 °C. The cone and desolvation gas flow were 50 L/h and 1000 L/h, respectively. Cone gas and collision gas were nitrogen and argon, respectively. Trap collision energy and transfer collision energy were off. Leucine enkephalin was used as a lock spray at a concentration of 200 pg/mL to ensure mass accuracy and reproducibility. This establishment was referenced in both positive mode at *m/z* 556.2771 $[M+H]^+$ and negative mode at *m/z* 554.2615 $[M\ H]^-$. The mass window was allowed to deviate 0.3 Da. The infusion flow rate of the lock spray was 10 μL/min. The scan time was every 60 s. MassLynx™ V4.1 software was used to operate the system. The data were analyzed by Progenesis QI (Waters Corp., Milford, USA), MarkerLynx™ XS (Waters Corp., Milford, USA), and MassFragment™ software (Waters Corp., Milford, USA). The significantly changed metabolites were filtered out based on VIP values

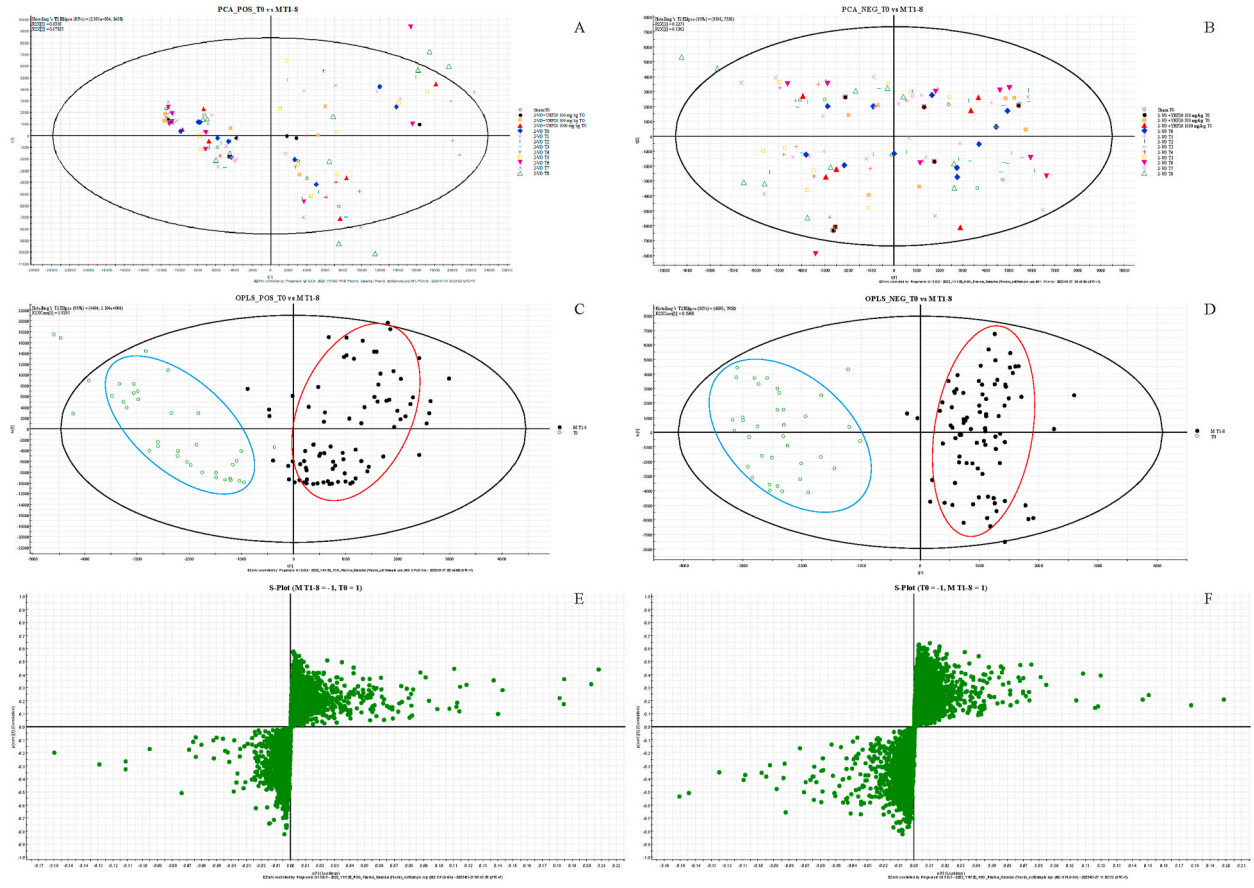

Fig. 2. Metabolic changes after ischemic-induced surgery at T0 compared to the 2-VO group at T1-T8; (A) PCA score plot in positive mode, (B) PCA score plot in negative mode, (C) OPLS-DA score plot in positive mode, (D) OPLS-DA score plot in negative mode, (E) S-plot in positive mode and (F) S-plot in negative mode.

(VIP>1), ANOVA ($P < 0.05$) and max fold change (≥2). The filtered metabolites were selected under special conditions; match score ≥40, mass error (ppm) close to 0 and highest mass fraction score. The chemical structures of important metabolites were then identified according to online databases such as the Human Metabolome Database (www.hmdb.ca), Metlin (www.metlin.scripps.edu) and the MassBank (www.massbank.jp) using the data of accurate masses and MS/MS fragments.

2.8. Morris water maze test

The Morris water maze was the behavioral test for spatial learning and memory after YHF20 or vehicle administrations (Fig. 1). The matt-black circle pool was 2.14 m in diameter and filled with water (20 ± 2 °C) to a depth of 0.25 m. The pool area was divided into 4 quadrants. The escape platform was a clear glass cylinder 9 cm in diameter. Visual cues were placed on the basin's edge, above the surface of the quadrant's four corners. Each one of them had a unique color and shape. In the experimental area, the least amount of light was allowed for monitoring and recording rat's behavior by a video camera above the pool [32]. SMART video tracking software v3.0 (Panlab, Spain) was used to analyze for speed and retention time.

2.9. Hepatotoxicity and nephrotoxicity analysis

The kidney and liver functions were assessed by BUN, creatinine (Cr), aspartate aminotransferase (AST), alanine aminotransferase (ALT), and alkaline phosphatase (ALP)-AMP, for acute (7 days) and subacute (28 days) drug toxicity study using automated biochemistry analyzer A15 (BioSystems, Barcelona, Spain).

Table 1
Known-tentative metabolic change that found in database.

No.	Metabolite	Formula	Mass error (ppm)	Database			Class
				HMDB	PubChem	KEGG	
1	L-Acetylcarnitine	C9H17NO4	−2.24	HMDB0000201	7,045,767	C02571	Fatty Acyls
2	Glutaurine	C7H14N2O6S	2.47	HMDB0004195	68,759	C05844	Carboxylic acids and derivatives
3	ELLIPTICINE	C17H14N2	3.10	HMDB0034310	–	–	Vinylogous acids
4	Genistein	C15H10O5	−1.36	HMDB0003217	5,280,961	C06563	Isoflavonoids
5	Naringenin	C15H12O5	−3.98	HMDB0002670	439,246	C00509	Flavonoids
6	O-oleoylcarnitine	C25H47NO4	0.20	HMDB0005065	46,907,933	–	Fatty Acyls
7	cinitapride	C21H30N4O4	1.93	HMDB0015698	68,867	–	Benzene and substituted derivatives
8	Ricinoleic Acid	C18H34O3	0.54	HMDB0034297	643,684	C08365	Fatty Acyls
9	3-dehydroecdysone	C27H42O6	−3.86	METPA1794	–	C02513	–
10	1-Tetradecanol	C14H30O	−1.79	HMDB0011638	8209	–	Fatty Acyls
11	Platelet-activating factor	C26H54NO7P	−1.09	METPA0517	–	C04598	–
12	1-Hydroxy-1-phenyl-3-hexadecanone	C22H36O2	−0.27	HMDB0035676	131,751,841	–	Fatty Acyls
13	FF-MAS	C29H46O	−1.25	HMDB0001023	443,212	C11455	Steroids and steroid derivatives
14	bilirubin	C33H36N4O6	0.78	HMDB0000054	21,252,250	C00486	Tetrapyrroles and derivatives
15	Azithromycin	C38H72N2O12	0.06	HMDB0014352	447,043	C06838	Organooxygen compounds
16	1-Palmitoyl-2-docosahexaenoyl-*sn*-glycero-3-phosphocholine	C46H80NO8P	1.97	HMDB0007991	6,441,886	C00157	Glycerophospholipids
17	PC(18:2 (9Z,12Z)/P-16:0)	C42H80NO7P	0.28	HMDB0008159	53,478,799	C00157	Glycerophospholipids
18	PC	C46H84NO8P	3.17	HMDB0000095	8117	C00055	Pyrimidine nucleotides
19	Glutathione	C20H32N6O12S2	−2.13	HMDB0062697	745	C00051	Carboxylic acids and derivatives
20	Carthamone	C21H20O11	−1.51	HMDB0037377	12,305,281	C08598	Cinnamic acids and derivatives
21	Baicalin	C21H18O11	−2.00	HMDB0041832	13,654,833	C10025	Flavonoids
22	glycochenodeoxycholic acid 7-sulfate	C26H43NO8S	−2.70	HMDB0002496	11,954,205	C01324	Homogeneous halogens
23	Glycodeoxycholic acid	C26H43NO5	−4.44	HMDB0000631	3,035,026	C05464	Steroids and steroid derivatives
24	Isodeoxycholic acid	C24H40O4	−3.85	HMDB0002536	164,672	C17661	Steroids and steroid derivatives
25	ruscogenin	C27H42O4	−0.76	–	441,893	C08909	steroidal saponins
26	Cyclopentadecanolide	C15H28O2	−2.82	HMDB0034455	235,414	–	Macrolides and analogues
27	4,6-Nonadecanedione	C19H36O2	−4.12	HMDB0035575	91,713,156	–	Organooxygen compounds
28	1D-myo-Inositol 1,2-cyclic phosphate	C6H11O8P	−2.89	HMDB0001125	122,331	C04299	Organic phosphoric acids and derivatives

2.10. Statistical analysis

All values in both the text and figures were expressed as mean ± standard deviation (SD) for n observations. When the data were normally distributed, one-way analysis of variance with Dunnett's post hoc test was performed using SPSS v.25 (IBM® SPSS® statistics, New York, USA), and p-values below 0.05 were considered to be significant. If the data were not normally distributed, Kruskal–Wallis H test or Friedman test were performed. p-values below 0.05 were considered to be significant. Graphs were plotted with GraphPad prism v.9 (Dotmatics, Boston, MA, USA).

3. Results

3.1. Identification of tentative biomarkers and pathway after BCCAO-induced ischemia

PCA and OPLS-DA were applied to compare metabolic changes after ischemic-induced surgery in all groups at T0 compared to the 2-VO group at T1-T8. As demonstrated by the PCA score plot in Fig. 2A–B, the difference between T0 of all groups versus 2-VO at T1-T8 was unclear in both modes. The R2X [1], R2X [2], R2X (cum) and Q2 (cum) were 0.64, 0.07, 0.93 and 0.85 in positive mode and were 0.22, 0.13, 0.82 and 0.59 in negative mode. Although, a clear separation was observed in the OPLS-DA score plot (Fig. 2C–D). The R2Y (cum) and Q2 (cum) were 0.75, 0.59 in positive mode and 0.90, 0.82 in negative mode. No overfitting was observed. The cutoff points were ±0.01 in S-plot (Fig. 2E–F). Subsequently, a total of 78 potential biomarkers including 39 changed metabolites in positive and 39 in negative mode were identified (Supplementary material, Table S2). There are 28 potential biomarkers which were found involved in various pathways using HMDB or Pubchem or KEGG database (Table 1).

28 metabolites were analyzed the potential pathways using MetaboAnalyst 5.0 (https://www.metaboanalyst.ca). The algorithm for pathways was hypergeometric test and relative-betweenness centrality selected for pathway enrichment analysis and topology analysis, respectively. The Homo sapiens from KEGG library was selected for this analysis. The overview of the matched pathway that arranged according to the scores from enrichment analysis (*y* axis) and from topology analysis (*x* axis) was shown in Fig. 3. The pathways have impact as glutathione metabolism, glycerophospholipid metabolism, ether lipid metabolism, steroid biosynthesis, porphyrin and chlorophyll metabolism, and pyrimidine metabolism. Glutathione metabolism has the highest impact that mainly the pathway associated with cerebral ischemia and/or dementia. The 78 tentative metabolites and 10 tentative pathways were used to identify the ischemic condition.

3.2. Metabolic changes after YHF20 administration

The tentative metabolites were analyzed the metabolic changes. The response of tentative metabolites was visualized using heatmap (Fig. 4). The results showed 7 known-tentative metabolites tended to change after pBCCAO-induced ischemia such glutathione, glutaurine, phosphatidylcholine (PC(16:0/16:0) or PC(18:2 (9Z, 12Z)/P-16:0)), FF-MAS, PC, platelet-activating factor and bilirubin (Fig. 5A–G) but not statistically significant difference between times. PC(16:0/16:0) tended to increase in 2-VO group at T1 and had decreasing trend in YHF20-treated group (Fig. 5B). N-Carbamimidoyl-4-hydrazinobenzenesulfonamide, that only significant increased in 2-VO group at T1 (7 days after pBCCAO-induced ischemia) compare with sham group, showed decreasing trend in YHF20-treated group (Fig. 5I).

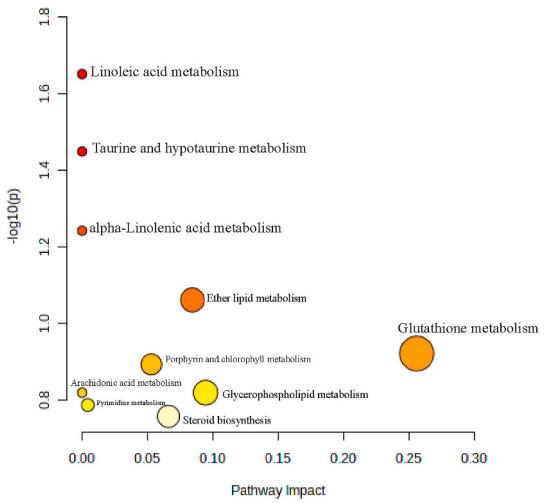

Fig. 3. The overview of pathway analysis from metabolic change after the BCCAO-induced ischemia.

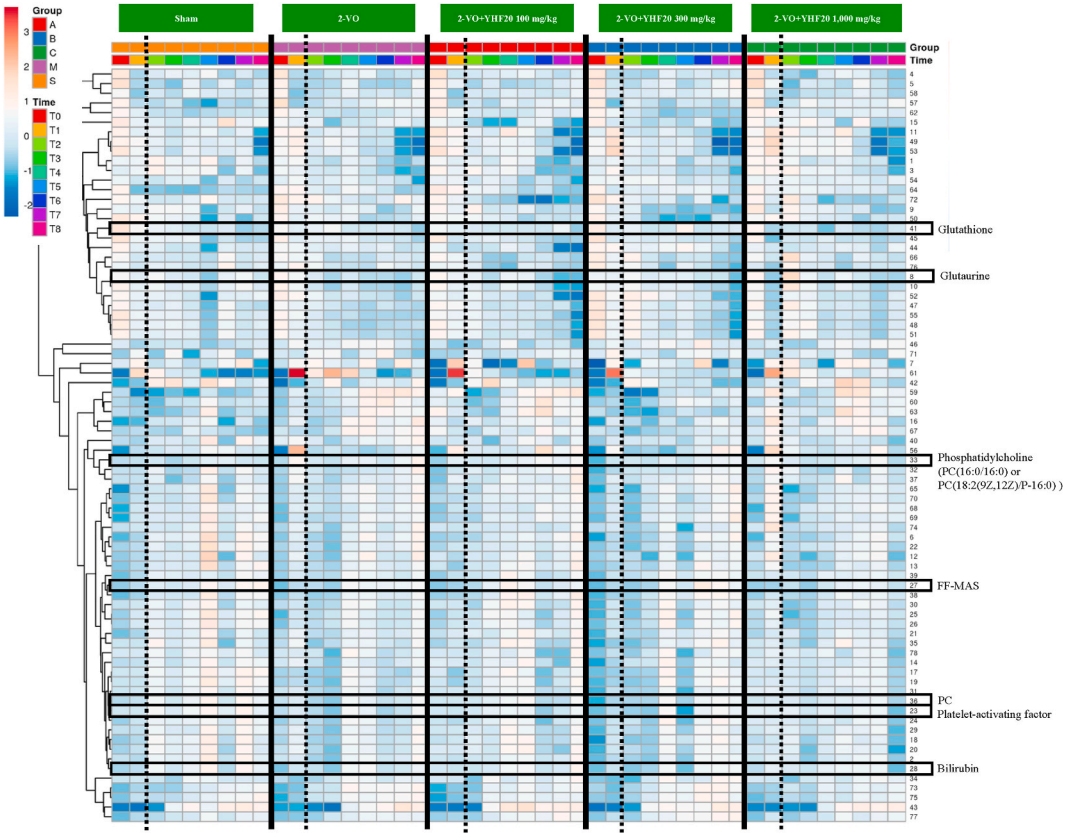

Fig. 4. The heatmap analysis of 78 differential metabolites identified between sham group, 2-VO group and 2-VO + YHF20-treated group. The vertical lines represent differential metabolites, and the horizontal lines represent group and time. The blue band indicates a decreased level of metabolite, and the red band indicates an increased level of metabolite.

3.3. Effect of YHF20 on spatial learning and memory performance

In the visible platform trial, the results showed a statistically significant difference in escape latency between the sham group and the 2-VO + YHF20 100 mg/kg group ($p = 0.03$). The swimming speed, distance to target and resting time were no statistically significant difference between all groups ($p = 0.82$, 0.19, 0.99, respectively) (Fig. 6A–D). These results indicated that visual and motor performances were not affected by pBCCAO. In the hidden platform trial, the results were a statistically significant between 2-VO and 2-VO + YHF20 100 mg/kg group in escape latency on day 1 ($p = 0.02$). The results showed a statistically significantly different between day 1 and day 5 in the sham group and all various doses of the YHF20-treated group, while the 2-VO group showed a statistically difference between day1 and day 3 (Fig. 6E). It indicates that the pBCCAO could not yet produce the impairment in spatial learning and memory which was induced by chronic cerebral ischemia hypoperfusion under this number of rats. Spatial memory retention was no statistically significant difference in mean retention time ($p = 0.38$) (Fig. 6F), swimming distance in the target quadrant ($p = 0.16$) (Fig. 6G) and latency to 1st entire target quadrant ($p = 0.58$) (Fig. 6H).

3.4. Toxicity after YHF20 administration

The hepatotoxicity and nephrotoxicity were not significantly different from sham group ($p > 0.05$) (Supplementary Material, Fig. S3). The weight change showed statistically significant difference between sham and 2-VO group on day 49, 56 and 71 ($p = 0.049$, 0.006, 0.007) and significant difference between sham and 2-VO + YHF20 100 mg/kg group on day 56 and 71 ($p = 0.046$, 0.006). (Supplementary Material, Fig. S3).

4. Discussion

In the present study, a non-targeted metabolomic approach based on LC-MS was performed to explore the characteristics of blood metabolism in rats with dementia. Cerebral ischemia hypoperfusion was induced by pBCCAO before 8 weeks of YHF20 administration. In metabolic profiling analysis, we identified 78 differentially expressed metabolites. Some metabolites had been reported in the progression of dementia such as L-Acetylcarnitine, Glutaurine, O-oleoyl carnitine [33,34]. The tentative metabolites were found in

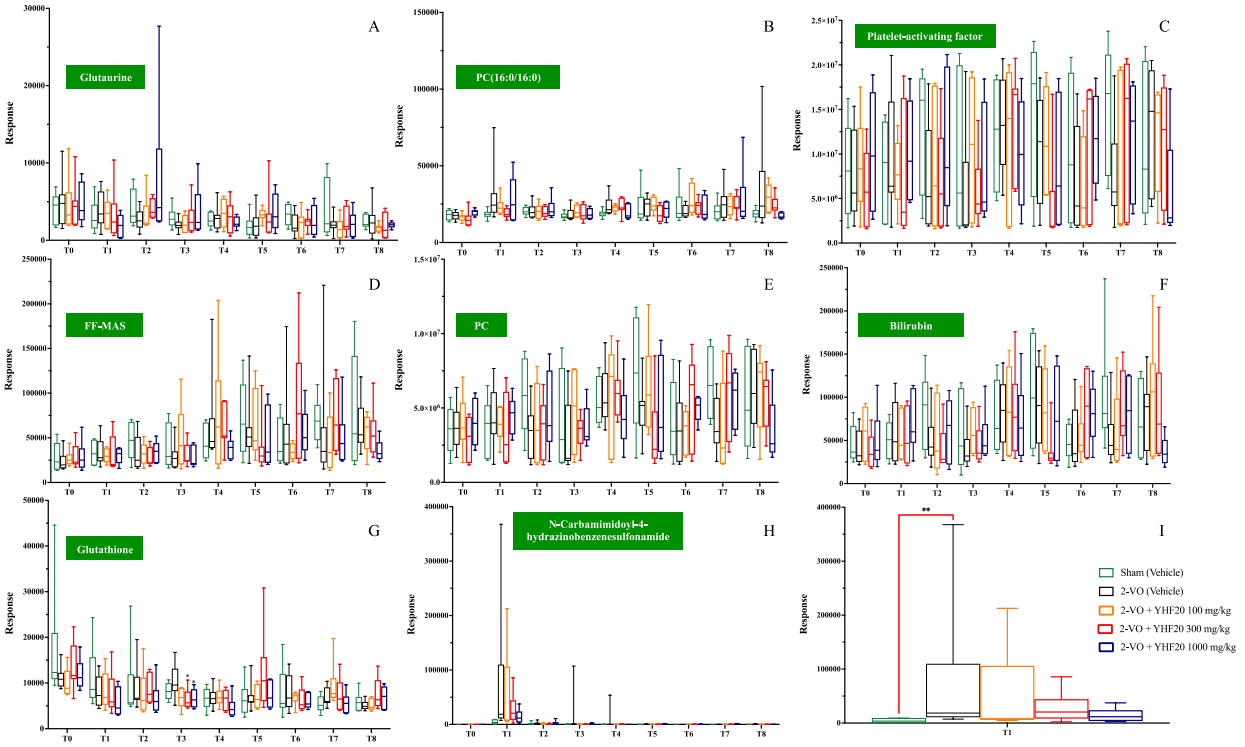

Fig. 5. Known metabolic change level; (A) Glutaurine (B) PC(16:0/16:0) (C) Platelet-activating factor (D) FF-MAS (E) PC (F) Bilirubin (G) Glutathione (H) N-Carbamimidoyl-4-hydrazinobenzenesulfonamide (I) N-Carbamimidoyl-4-hydrazinobenzenesulfonamide at T1. *p < 0.05 compared with 2-VO group; **p < 0.01 compared with 2-VO group.

2-VO group but not sham group may be the potential biomarkers of cerebral ischemia hypoperfusion especially N-Carbamimidoyl-4-hydrazinobenzenesulfonamide. However, there is no report about N-Carbamimidoyl-4-hydrazinobenzenesulfonamide pharmacological activity related to cerebral ischemia. The identified potential biomarkers were screened according to the FDR of significance. These biomarkers by pathway topology analysis were primarily involved in the metabolism of taurine and hypotaurine metabolism, alpha-linolenic acid metabolism, ether lipid metabolism, glutathione metabolism, porphyrin and chlorophyll metabolism, arachidonic acid metabolism, glycerophospholipid metabolism, pyrimidine metabolism, steroid biosynthesis as many previous studies [35–38]. Therefore, our results revealed that cerebral ischemia hypoperfusion could cause cognitive impairment by affecting a variety of metabolic pathways mainly in glutathione metabolism. Glutathione metabolism links to glutathione metabolite that play role in antioxidant defense and regulation of cellular events [39]. Glutathione can suppress cerebral infarct volume and cell death after ischemic injury [40]. Nevertheless, this study was a non-target metabolomics study. The results were potential biomarkers that have not been studied for pharmacological activity. In the future, extraction methods should be developed to quantify these compounds or analyze their activity as target metabolomics studies such as the effect of YHF20 on glutathione level.

Spatial learning and memory could be determined by many tasks, such as the spatial object recognition (SOR) test, Radial arm maze, Y-maze, Barnes maze and Morris water maze (MWM). This study chose the MWM to evaluate the effect of YHF20 on spatial learning and memory. The initial assessment involved evaluating sensorimotor performance in the visible platform trial that monitored escape latency and swimming speed. Swimming speed of 2-VO group and 2-VO + YHF20-treated groups were not different from sham group indicated the normal motor performance. However, it was observed that the 2-VO+100 mg/kg YHF20 group exhibited high escape latency and a greater distance from the target, suggesting thigmotaxis behavior which is often associated with anxiety or stress in rats, leading to spending more time along the pool wall [18,41].

During the acquisition trial, the 2-VO group showed less decreases of escape latency as compared to the sham group but was not statistically significant when compared within same day (Fig. 6E). The wide standard deviation might cause the non-significant different results and a greater number of rats might be needed to cover the behavioral variation. The minimum number of rats was 10, indicating the difference between the sham group and the 2-VO group [42]. Further study may increase number of rats in experimental period and add a positive control to confirm the success of treatment in this ischemic or learning and memory deficit model during the method validation. In addition, cognitive deficit should be confirmed the occurrence of the cerebral ischemia hypoperfusion by measuring the numbers of surviving hippocampal neurons (CA1, CA3 and dentate gyrus) and grading the white matter injury.

Therefore, the effect of YHF20 was considered to be compared by the intragroup change values. YHF20 has been used in Thai traditional medicine. Some components had been reporting pharmacological effects but there was no evidence the effect of YHF20

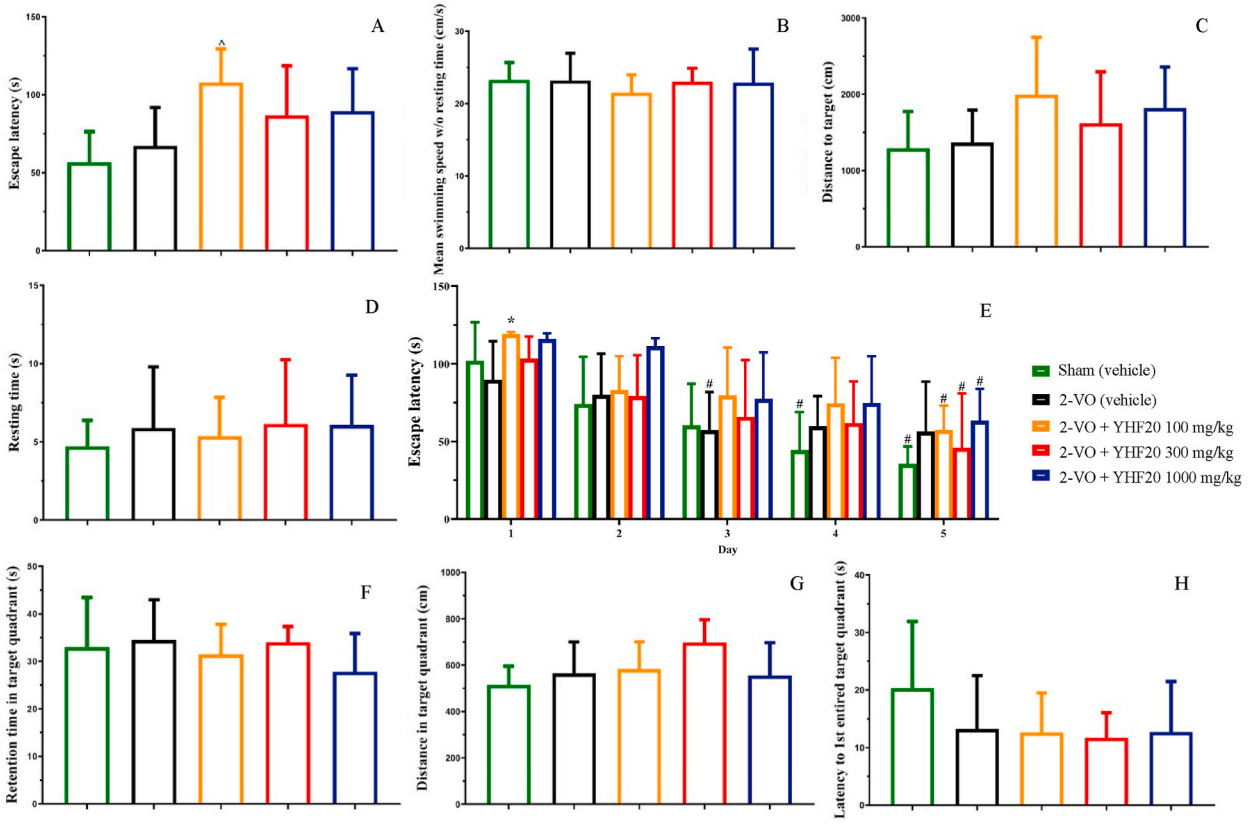

Fig. 6. Spatial learning and memory performance after YHF20 administration; (A) escape latency, (B) mean swimming speed without resting time, (C) distance to target, (D) resting time, (E) escape latency of hidden platform trial, (F) retention time in target quadrant, (G) distance in target quadrant, (H) latency to 1st entired target quadrant. ˆp < 0.05 compared with sham group; *p < 0.05 compared with 2-VO group in the same day; #p < 0.05 compared with day1 in the same group.

against the cerebral ischemia. In this study, sham group and YHF20-treated groups showed a statistically significant change in escape latency between day 1 and day 5 in the acquisition trial. All YHF20-treated groups tended to cause more decreases in escape latency than the 2-VO group on day 5. After the competition of the acquisition trial, the retention of spatial memory was assessed in probe trial. The data showed no difference of retention time in target quadrant between any groups and sham group tended to use more time to 1st entired the target quadrant. However, 2-VO+300 mg/kg YHF20 group tended to be more distant in target quadrant than other groups that indicated rats might remember the platform position.

Another potential issue with the MWM is that the period after 2-VO also plays a role in evaluating spatial learning and memory impairment. Various times after the 2-VO procedure were chosen from 30 to 90 days [43–45]. The previous study showed arteriogenesis in the vertebrobasilar tree to recover cerebral blood flow and signs of optic tract degeneration after 3 months [46] and reported the significant different escape latency at 8 weeks from 1 to 3 weeks [47]. Likewise, this study chose 2 months after 2-VO corresponded to YHF20 was usually consecutively used for 1–3 months ago in clinical practice.

YHF20 is a herbal formula regularly used in the Ayurved Siriraj Clinic of Thai traditional medicine to improve symptoms resulting from wind element obstruction in the upper region of the body, such as nausea, vomiting, dizziness and exhaustion. According to Thai traditional medicine theory, YHF20 has a gentle taste that can regulate wind element to restore normal blood flow. Cerebral blood flow deficiency for brain metabolism leads to cerebral ischemia and the development of vascular dementia. Many compounds have been reported in the component of YHF20 which relate to attenuate the cerebral ischemic injury such as antioxidation, anti-inflammatory effect, anti-ischemic effect. This study found 4 tentative metabolites may be the metabolites of YHF20's constituents including genistein, naringenin, baicalin and ruscogenin. Genistein downregulate the expression of nod-like receptor protein 3 (NLRP3) inflammasome, decreased inflammatory factor release and regulate the mitochondria-dependent apoptosis pathways [48–50]. Naringenin can inhibit oxidative stress and inflammation [51,52]. Baicalin can attenuate ischemia-induced neuronal cell damage via anti-oxidative and anti-apoptotic effect [53,54]. Ruscogenin also suppress thiredoxin-interactive protein (TXNIP) and NLRP3 inflammasome activation. Therefore, the effect YHF20 on vascular system are required in the future investigation.

This study had limitations that could be addressed in future research. First, the cerebral ischemia condition confirmation might directly measure using histological staining [55,56], Immunofluorescence analysis [55–57], brain-derived neurotrophic factor (BDNF) level [58,59]. Then, this can be indirectly measure by inflammatory cytokines detection [60,61] and oxidative stress assessment [56,

61]. Second, increasing of the sample size to at least 10 will improve the accuracy of the behavioral result and avoid erroneous conclusions. However, this study is the first to examine how YHF20 affects rats after neural damage. It was discovered that YHF20 can change metabolites associated with pathways which occur during cerebral ischemia. Furthermore, these findings can serve as the groundwork for evidence-based medicine in future studies. These entails developing a method for determining a targeted metabolic change and performing in vitro tests using anti-inflammatory, antioxidant evaluations to provide information for investigating the metabolic pathways of YHF20.

5. Conclusion

In this study, the permanent bilateral common carotid artery occlusion for 2 months was not interfering the learning and memory performance (n = 6–11). Although, the administration of the various dose of YHF20 has not been able to conclude the effect on spatial learning and memory impairment but might contribute in metabolic changes related to cerebral ischemia condition. Glutathione and glutathione metabolism may be the metabolic path affected by YHF20. The 4 identified metabolites which might be the metabolites from the components of YHF20 can be taken into consideration and verified for quality control. No toxicity was observed after the YHF20 administration for 56 days.

Ethics statement

All experimental protocols were approved by the Siriraj Animal Care and Use Committee (SiACUC), Faculty of Medicine Siriraj Hospital, Mahidol University. (COA No. 002/2559).

Funding statement

This research was made possible through the generous financial support of the Siriraj Research Development Fund, grant number R016032004, Faculty of Medicine Siriraj Hospital, Mahidol University, Thailand.

Data availability statement

Data included in article/supplementary material/referenced in article.

CRediT authorship contribution statement

Pravit Akarasereenont: Writing – review & editing, Methodology, Conceptualization. **Saracha Pattanapholkornsakul:** Writing – original draft, Methodology, Formal analysis, Data curation. **Suveerawan Limsuvan:** Writing – original draft, Data curation. **Dollaporn Mamaethong:** Writing – original draft, Data curation. **Suksalin Booranasubkajorn:** Writing – review & editing, Formal analysis, Data curation. **Narawut Pakaprot:** Writing – review & editing, Methodology, Conceptualization. **Pinpat Tripatara:** Writing – review & editing, Methodology, Conceptualization. **Kajee Pilakasiri:** Writing – review & editing, Methodology, Conceptualization.

Declaration of competing interest

The authors declare that they have no known competing financial interests or personal relationships that could have appeared to influence the work reported in this paper.

Acknowledgement

We acknowledge the Centre of Applied Thai Traditional Medicine and the Department of Pharmacology, Faculty of Medicine Siriraj Hospital, Mahidol University, Thailand, for providing a conducive research environment and access to necessary resources. For the recommendation and experimental supports, the authors are grateful to Dr. Manmas Vannabhum, Mr. Sukit Huabprasert, Ms. Pruksa Chotitham and Ms. Namphung Thongta. All authors sincerely appreciate your contribution.

Appendix A. Supplementary data

Supplementary data to this article can be found online at https://doi.org/10.1016/j.heliyon.2024.e28027.

References

[1] J.H. Garcia, G.G. Brown, Vascular dementia: neuropathologic alterations and metabolic brain changes, J. Neurol. Sci. 109 (2) (1992) 121–131.
[2] P. Scheel, et al., Volume reduction in cerebral blood flow in patients with vascular dementia, Lancet 354 (9196) (1999) 2137.

[3] M. Sopala, W. Danysz, Chronic cerebral hypoperfusion in the rat enhances age-related deficits in spatial memory, J. Neural. Transm. 108 (12) (2001) 1445–1456.
[4] E. Farkas, P.G. Luiten, F. Bari, Permanent, bilateral common carotid artery occlusion in the rat: a model for chronic cerebral hypoperfusion-related neurodegenerative diseases, Brain Res. Rev. 54 (1) (2007) 162–180.
[5] J. Duncombe, et al., Chronic cerebral hypoperfusion: a key mechanism leading to vascular cognitive impairment and dementia. Closing the translational gap between rodent models and human vascular cognitive impairment and dementia, Clin. Sci. (Lond.) 131 (19) (2017) 2451–2468.
[6] R.J. Traystman, Animal models of focal and global cerebral ischemia, ILAR J. 44 (2) (2003) 85–95.
[7] M.Z. Othman, Z. Hassan, A.T. Che Has, Morris water maze: a versatile and pertinent tool for assessing spatial learning and memory, Exp. Anim. 71 (3) (2022) 264–280.
[8] N. B, et al., The relationship between erythropoietin pretreatment with blood-brain barrier and lipid peroxidation after ischemia/reperfusion in rats, Life Sci. 80 (14) (2007) 1245–1251.
[9] S.S. Chan, T.Y. Cheng, G. Lin, Relaxation effects of ligustilide and senkyunolide A, two main constituents of Ligusticum chuanxiong, in rat isolated aorta, J. Ethnopharmacol. 111 (3) (2007) 677–680.
[10] X.L. Chang, et al., [Studies on chemical constituents of rhizomes of Ligusticum chuanxiong], Zhongguo Zhongyao Zazhi 32 (15) (2007) 1533–1536.
[11] A. Dar, et al., Hypotensive effect of the methanolic extract of Mimusops elengi in normotensive rats, Phytomedicine 6 (5) (1999) 373–378.
[12] H.P. Madlala, et al., Changes in Renal function and oxidative Status associated with the Hypotensive effects of oleanolic acid and related Synthetic Derivatives in experimental animals, PLoS One 10 (6) (2015) e0128192.
[13] P. Nyadjeu, et al., Antihypertensive and vasorelaxant effects of Cinnamomum zeylanicum stem bark aqueous extract in rats, J. Compl. Integr. Med. 8 (2011).
[14] L.O. Somova, et al., Cardiovascular, antihyperlipidemic and antioxidant effects of oleanolic and ursolic acids in experimental hypertension, Phytomedicine 10 (2–3) (2003) 115–121.
[15] C.E. Damiani, L.V. Rossoni, D.V. Vassallo, Vasorelaxant effects of eugenol on rat thoracic aorta, Vasc. Pharmacol. 40 (1) (2003) 59–66.
[16] S. Adefegha, G. Oboh, In vitro inhibition activity of polyphenol-rich extracts from Syzygium aromaticum (L.) Merr. & Perry (Clove) buds against carbohydrate hydrolyzing enzymes linked to type 2 diabetes and Fe(2+)-induced lipid peroxidation in rat pancreas, Asian Pac. J. Trop. Biomed. 2 (10) (2012) 774–781.
[17] A. Chanwitheesuk, A. Teerawutgulrag, N. Rakariyatham, Screening of antioxidant activity and antioxidant compounds of some edible plants of Thailand, Food Chem. 92 (2005) 491–497.
[18] Y. Huang, W. Zhou, Y. Zhang, Bright lighting conditions during testing increase thigmotaxis and impair water maze performance in BALB/c mice, Behav. Brain Res. 226 (1) (2012) 26–31.
[19] H.A. Jung, et al., Antioxidant principles of Nelumbo nucifera stamens, Arch Pharm. Res. (Seoul) 26 (4) (2003) 279–285.
[20] A. Manosroi, et al., Anti-proliferative and matrix metalloproteinase-2 inhibition of Longkong (Lansium domesticum) extracts on human mouth epidermal carcinoma, Pharm. Biol. 51 (10) (2013) 1311–1320.
[21] Sindhu Mathew, T.E. Abraham, Studies on the antioxidant activities of cinnamon (Cinnamomum verum) bark extracts, through various in vitro models, Food Chem. 94 (4) (2006) 520–528.
[22] D. Shahwar, M.A. Raza, Antioxidant potential of phenolic extracts of Mimusops elengi, Asian Pac. J. Trop. Biomed. 2 (7) (2012) 547–550.
[23] N.P. Visavadiya, B. Soni, N. Dalwadi, Evaluation of antioxidant and anti-atherogenic properties of Glycyrrhiza glabra root using in vitro models, Int. J. Food Sci. Nutr. 60 (Suppl 2) (2009) 135–149.
[24] B.C. S, M. R, Post-ischemic administration of nimodipine following focal cerebral ischemic-reperfusion injury in rats alleviated excitotoxicity, neurobehavioural alterations and partially the bioenergetics, Int. J. Dev. Neurosci. 29 (1) (2011) 93–105.
[25] X. Chu, et al., Licochalcone a inhibits lipopolysaccharide-induced inflammatory response in vitro and in vivo, J. Agric. Food Chem. 60 (15) (2012) 3947–3954.
[26] M.H. Duan, et al., Angelica sinensis reduced Abeta-induced memory impairment in rats, J. Drug Target. 24 (4) (2016) 340–347.
[27] S.D. Gopalakrishnan C, S.K. Nazimudeen, S. Viswanathan, L. Kameswaran, Anti-inflammatory and C.N.S. depressant activities of xanthones from Calophyllum inophyllum and Mesua ferrea, Indian J. Pharmacol. 12 (3) (1980) 181–191.
[28] H.K. Kim, et al., Down-regulation of iNOS and TNF-alpha expression by kaempferol via NF-kappaB inactivation in aged rat gingival tissues, Biogerontology 8 (4) (2007) 399–408.
[29] K. Likhitwitayawuid, K. Sawasdee, K. Kirtikara, Flavonoids and stilbenoids with COX-1 and COX-2 inhibitory activity from Dracaena loureiri, Planta Med. 68 (9) (2002) 841–843.
[30] P. Thiyagarajan, et al., Modulation of lipopolysaccharide-induced pro-inflammatory mediators by an extract of Glycyrrhiza glabra and its phytoconstituents, Inflammopharmacology 19 (4) (2011) 235–241.
[31] Sachin Vetal, et al., Anti-inflammatory and anti-arthritic activity of type-A procyanidine polyphenols from bark of Cinnamomum zeylanicum in rats, Food Sci. Hum. Wellness 2 (2) (2013) 59–67.
[32] R. Morris, Developments of a water-maze procedure for studying spatial learning in the rat, J. Neurosci. Methods 11 (1) (1984) 47–60.
[33] R. C, et al., Blood metabolite markers of preclinical Alzheimer's disease in two longitudinally followed cohorts of older individuals, Alzheimers Dement 12 (7) (2016) 815–822.
[34] J. Li, et al., Metabolic profiling of the effects of ginsenoside Re in an Alzheimer's disease mouse model, Behav. Brain Res. 337 (2018) 160–172.
[35] M. A, et al., Glutathione Peroxidase activity is altered in vascular cognitive impairment-No dementia and is a potential Marker for Verbal memory performance, J Alzheimers Dis 79 (3) (2021) 1285–1296.
[36] M. Zabel, et al., Markers of oxidative damage to lipids, nucleic acids and proteins and antioxidant enzymes activities in Alzheimer's disease brain: a meta-analysis in human pathological specimens, Free Radic. Biol. Med. 115 (2018) 351–360.
[37] Y. Jiang, et al., Metabolomics in the development and progression of dementia: a Systematic review, Front. Neurosci. 13 (2019) 343.
[38] M. Schrag, et al., Oxidative stress in blood in Alzheimer's disease and mild cognitive impairment: a meta-analysis, Neurobiol. Dis. 59 (2013) 100–110.
[39] G. Wu, et al., Glutathione metabolism and its implications for health, J. Nutr. 134 (3) (2004) 489–492.
[40] J. Song, et al., Glutathione suppresses cerebral infarct volume and cell death after ischemic injury: involvement of FOXO3 inactivation and Bcl2 expression, Oxid. Med. Cell. Longev. 2015 (2015) 426069.
[41] Anjanette P. Harris, Richard B. D'Eath, S.D. Healy, Environmental enrichment enhances spatial cognition in rats by reducing thigmotaxis (wall hugging) during testing, Anim. Behav. 77 (6) (2009) 1459–1464.
[42] D. B, et al., Watermaze performance after middle cerebral artery occlusion in the rat: the role of sensorimotor versus memory impairments, J. Cerebr. Blood Flow Metabol. 32 (6) (2012) 989–999.
[43] F. Cechetti, et al., Forced treadmill exercise prevents oxidative stress and memory deficits following chronic cerebral hypoperfusion in the rat, Neurobiol. Learn. Mem. 97 (1) (2012) 90–96.
[44] T. Damodaran, et al., Time course of motor and cognitive functions after chronic cerebral ischemia in rats, Behav. Brain Res. 275 (2014) 252–258.
[45] X. Song, et al., Protective effect of Daming capsule against chronic cerebral ischemia, BMC Compl. Alternative Med. 15 (2015) 149.
[46] G. Soria, et al., The ins and outs of the BCCAo model for chronic hypoperfusion: a multimodal and longitudinal MRI approach, PLoS One 8 (9) (2013) e74631.
[47] K. Thong-asa, et al., Reversible short-term and delayed long-term cognitive impairment induced by chronic mild cerebral hypoperfusion in rats, J. Neural. Transm. 120 (8) (2013) 1225–1235.
[48] Y. Qian, et al., Neuroprotection by the soy isoflavone, genistein, via inhibition of mitochondria-dependent apoptosis pathways and reactive oxygen induced-NF-kappaB activation in a cerebral ischemia mouse model, Neurochem. Int. 60 (8) (2012) 759–767.
[49] S. Wang, et al., Genistein attenuates acute cerebral ischemic damage by inhibiting the NLRP3 inflammasome in Reproductively Senescent mice, Front. Aging Neurosci. 12 (2020) 153.
[50] Y.X. Wang, et al., Genistein inhibits hypoxia, ischemic-induced death, and apoptosis in PC12 cells, Environ. Toxicol. Pharmacol. 50 (2017) 227–233.

[51] P. Zhao, Y. Lu, Z. Wang, Naringenin attenuates cerebral ischemia/reperfusion injury by inhibiting oxidative stress and inflammatory response via the activation of SIRT1/FOXO1 signaling pathway in vitro, Acta Cir. Bras. 38 (2023) e380823.
[52] S.S. Raza, et al., Neuroprotective effect of naringenin is mediated through suppression of NF-kappaB signaling pathway in experimental stroke, Neuroscience 230 (2013) 157–171.
[53] Y. Cao, et al., Baicalin attenuates global cerebral ischemia/reperfusion injury in gerbils via anti-oxidative and anti-apoptotic pathways, Brain Res. Bull. 85 (6) (2011) 396–402.
[54] Q.B. Zhou, et al., Baicalin attenuates focal cerebral ischemic reperfusion injury by inhibition of protease-activated receptor-1 and apoptosis, Chin. J. Integr. Med. 20 (2) (2014) 116–122.
[55] L. Zheng, et al., Pentoxifylline alleviates ischemic white matter injury through up-regulating Mertk-mediated myelin clearance, J. Neuroinflammation 19 (1) (2022) 128.
[56] Q. Xiao, et al., Bushen-Yizhi formula exerts neuroprotective effect via inhibiting excessive mitophagy in rats with chronic cerebral hypoperfusion, J. Ethnopharmacol. 310 (2023) 116326.
[57] F. Zhao, et al., Untargeted metabolomics uncovering neuroprotective effect of Dl-3-n-butylphthalide on improving cognitive impairment induced by chronic cerebral hypoperfusion in rats, Int. Immunopharm. 119 (2023) 110271.
[58] M. To, et al., Cognitive Dysfunction in a mouse model of cerebral ischemia influences Salivary metabolomics, J. Clin. Med. 10 (8) (2021).
[59] S. Bathina, U.N. Das, Brain-derived neurotrophic factor and its clinical implications, Arch. Med. Sci. 11 (6) (2015) 1164–1178.
[60] F. Yan, et al., Xi-Xian-Tong-Shuan capsule alleviates vascular cognitive impairment in chronic cerebral hypoperfusion rats by promoting white matter repair, reducing neuronal loss, and inhibiting the expression of pro-inflammatory factors, Biomed. Pharmacother. 145 (2022) 112453.
[61] M. Kaundal, R. Deshmukh, M. Akhtar, Protective effect of betulinic acid against intracerebroventricular streptozotocin induced cognitive impairment and neuronal damage in rats: possible neurotransmitters and neuroinflammatory mechanism, Pharmacol. Rep. 70 (3) (2018) 540–548.